Skolkovo Institute of Science and Technology

Center for Design, Manufacturing and Materials

Thermal Fluid Sciences

Term 3, Course Project #1:

Liquid Flow Through in Pipe

Instructor: Prof. Iskander Akhatov

TA: Radmir Karamov

Students:

Anastasia Cumika, 2nd year MSc student, CDMM

Oleg Nikolaev, 1st year MSc student, CHR

Ruslan Vorobyev, 3rd year PhD student, CDMM

Moscow, Russia

2021

Presentation Plan

- ➔ Introduction, Literature Review & Practical Importance
- ➔ Problem statement
- ➔ Analytical Solution
- ➔ Numerical Solution
- ➔ Results
- ➔ Discussion & Future Efforts

Introduction

➔ Simulation of laminar, transient and turbulent flow will be conducted for this project

➔ Axial velocity profiles and volumetric flow rate will be analyzed

➔ Computational Fluid Dynamics (CFD) for velocity profile will be compared to analytical fluid dynamics

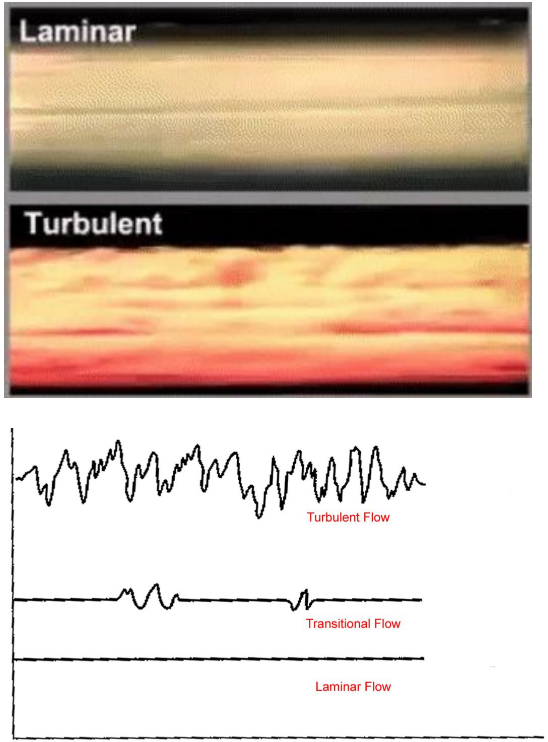

Fig. 1. Flow visualization of transition from laminar to turbulent.

Source: Sawicki, Jerzy. (1997). Mechanics of pollutants transfer.

Literature Review

Table 1. List of literature used for analysis of the problem.

Source	**Notes**
Munson et al, *"Fundamentals of Fluid Mechanics, 7th Edition"*, Chapter 8: Viscous Flow in Pipes, 2021	● identify and understand various characteristics of the flow in pipes; ● discuss the main properties of laminar and turbulent pipe flow and appreciate their differences; ● apply appropriate equations and principles to analyze a variety of pipe flow situations.
Farsirotou et al, "*Experimental investigation of fluid flow in horizontal pipes system of various cross-section geometries.*" EPJ Web of Conferences. 67. 10.1051/epjconf/20146702026, 2014	Experimental validation of the studied materials
Adamkowski, "*Analysis of Transient Flow in Pipes With Expanding or Contracting Sections*". Journal of Fluids Engineering-transactions of The Asme - J FLUID ENG. 125. 10.1115/1.1593703, 2014	Mathematical modeling of transient flow in pipes
ANSYS & FlowVision Documentation	Used models and formulations and their agreement with theoretical and numerical calculations of viscous media

Practical Importance

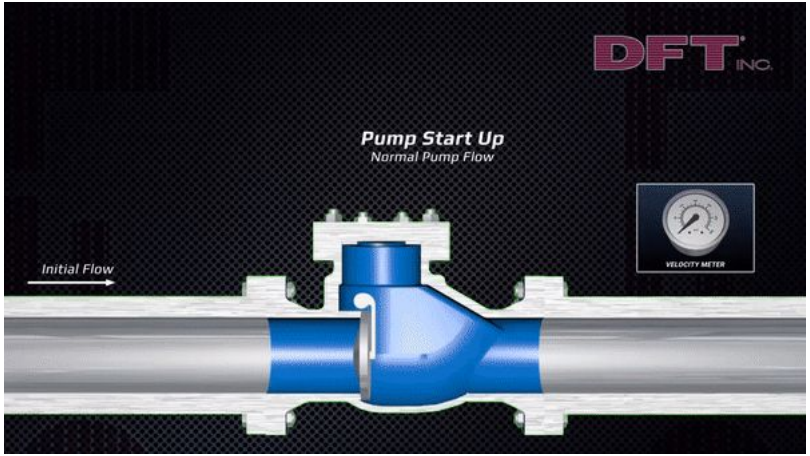

Fig. 2. Example of transient flow occurring within check valve.

Fig. 3. Possible effect of lack of proper calculation.

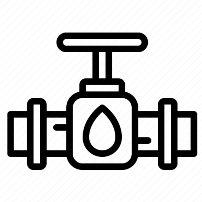

Oil & Gas

Hydroelectric
Power Stations

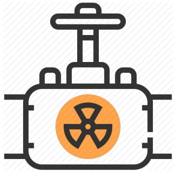

Nuclear Power
Plants

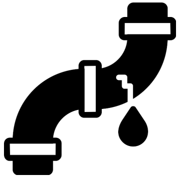

and more
others...

Source: What is Water Hammer? | DFT Inc.; https://www.ishn.com/articles/108930-fatigue-crack-cause-of-pipeline-rupture-oil-spill

Problem Statement

Viscous liquid (μ=2×10^{-2} kg/m×s, r=0.9×10^{3} kg/m^{3}) is initially at rest in the cylindrical pipe of diameter D = 8 cm and length L = 1.2 m. Constant pressure gradient is applied at the moment t = 0. Use ANSYS. Calculate transient flow until it becomes steady. Compare the numerical results with analytical solution of the problem, if any. First, select pressure gradient low enough so that the steady flow is laminar. Second, increase pressure gradient to get instability in the flow and match the result with the Moody chart. Explore dependency of the solution on all parameters.

Assumptions:

- Newtonian, incompressible, isotropic liquid;
- Smooth pipe (friction neglected);

$$\mu = 2 \cdot 10^{-2}\ kg/m \cdot s$$

$$\rho = 0.9 \cdot 10^{3}\ kg/m^{3}$$

$$D = 8\ cm, L = 1.2\ m$$

$$\begin{cases} v = 0, \ \ t = 0 \\ v(t,r), \ \ t > 0\ (P_1 > P_2\ applied) \end{cases}$$

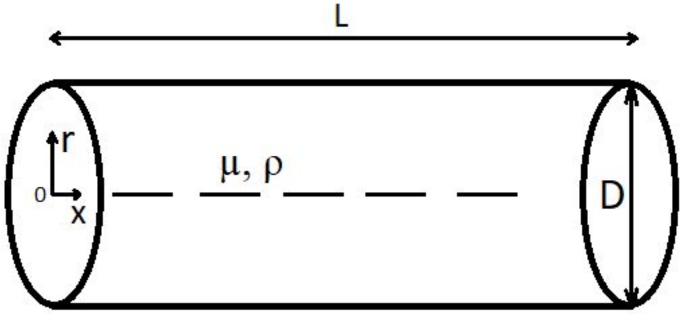

Fig. 4. Problem statement illustration.

Analytical solution

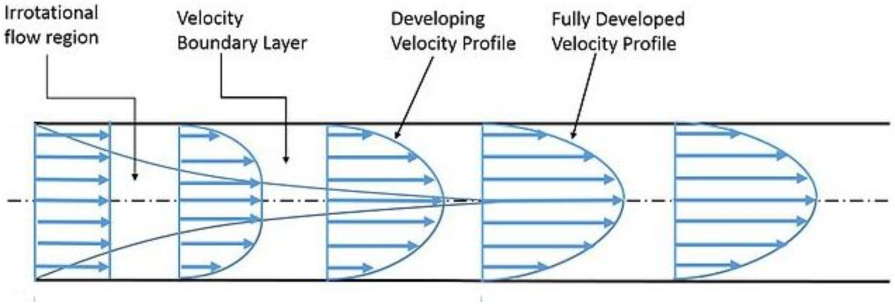

Fig. 5. Flow development in time

PDE method

$$\frac{\partial v}{\partial t} = \frac{\mu}{\rho}\left(\frac{\partial^2 v}{\partial r^2} + \frac{1}{r}\frac{\partial v}{\partial r}\right) - \frac{1}{\rho}\frac{\partial P}{\partial x}$$

Navier–Stokes equation

$$-\frac{1}{\rho}\frac{\partial P}{\partial x} = \frac{P_1 - P_2}{\rho L} = \frac{G}{\rho}$$

G - pressure gradient

New function:

$$w(t,r) = \underbrace{\frac{G}{4\mu}(R^2 - r^2)}_{\text{Poiseuille's law}} - v(r,t)$$

$$\begin{cases} \dfrac{\partial w}{\partial t} = \nu\left(\dfrac{\partial^2 w}{\partial r^2} + \dfrac{1}{r}\dfrac{\partial w}{\partial r}\right) \\ w(t,R) = 0 \\ w(0,r) = \dfrac{G}{4\mu}(R^2 - r^2) \end{cases}$$

boundary equation

initial condition

Fourie method: $w(t,r) = W(r)T(t)$

$$WT' = \nu\left(W'' + \frac{1}{r}W'\right)T$$

$$\frac{T'}{\nu T} = \frac{W'' + \frac{1}{r}W'}{W}$$

Analytical solution

$$\frac{T'}{\nu T} = \frac{W'' + \frac{1}{r}W'}{W} = -a^2 < 0$$

$$W'' + \frac{1}{r}W' + a^2 W = 0$$

$$\frac{1}{a^2}\frac{d^2W}{dr^2} + \frac{1}{ar}\frac{1}{a}\frac{dW}{dr} + W = 0$$

$$ar = \xi$$

$$\frac{d^2W}{d\xi^2} + \frac{1}{\xi}\frac{dW}{d\xi} + W = 0$$

$$w(t,r) = C \cdot \exp\left(-\nu a^2 t\right)\underbrace{J_0(ar)}_{\text{Bessel equation of zero order}}$$

$$w(t,R) = 0 \to J_0(aR) = 0$$

$$a_n R = \lambda_n\,, a_n = \frac{\lambda_n}{R}$$

$$J_0(\lambda_n) = 0$$

$$\frac{T'}{T} = -\nu a^2$$

$$T = C_1 \cdot \exp\left(-\nu a^2 t\right)$$

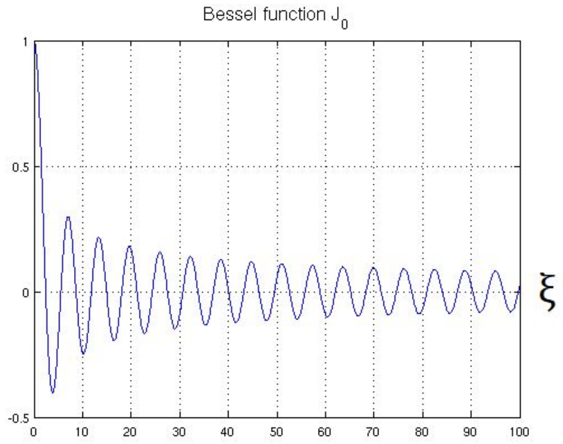

Fig. 6. Bessel function zeros

Jean-Baptiste Joseph Fourier
1768 – 1830

$$w(t,r) = C_n \cdot \exp(-\nu {a_n}^2 t) J_0(a_n r) = C_n \cdot \exp\left(-\nu \frac{{\lambda_n}^2 t}{R}\right) J_0\left(\lambda_n \frac{r}{R}\right)$$

for $\exists C_n$ satisfying eq of B. C. on the wall

$$\boxed{w(t,r) = \sum_{n=1}^{\infty} C_n \cdot \exp(-\nu {a_n}^2 t) J_0\left(\lambda_n \frac{r}{R}\right)}$$

Analytical solution

$$w(t,r) = \sum_{n=1}^{\infty} C_n \cdot \exp(-\nu a_n{}^2 t) J_0\left(\lambda_n \frac{r}{R}\right)$$

$$t = 0: w(0,r) = \frac{G}{4\mu}(R^2 - r^2) = \sum_{n=1}^{\infty} C_n \cdot J_0\left(\lambda_n \frac{r}{R}\right)$$

$$\int_0^{\infty} 2\pi r J_0\left(\lambda_n \frac{r}{R}\right) J_0\left(\lambda_m \frac{r}{R}\right) dr = \sigma_{nm}$$

$$C_n = \frac{G}{4\mu} \frac{8R^2}{\lambda_n{}^3 J_1(\lambda_n)}$$

$$\boxed{\begin{aligned} v(t,r) &= \frac{G}{4\mu}(R^2 - r^2) - \frac{2GR^2}{\mu} \sum_{n=1}^{\infty} \frac{J_0\left(\lambda_n \frac{r}{R}\right)}{\lambda_n{}^3 J_1(\lambda_n)} \exp\left(-\nu \frac{\lambda_n{}^2 t}{R^2}\right) \\ Q(t) &= \frac{\pi G R^2}{8\mu}\left[1 - 32 \sum_{n=1}^{\infty} \frac{1}{\lambda_n{}^4} \exp\left(-\nu \frac{\lambda_n{}^2 t}{R^2}\right)\right] \end{aligned}}$$

Analytical solution

Dimensionless analysis

$$r_D = \frac{r}{R} \qquad t_D = \frac{\nu t}{R^2} \qquad v_D = \frac{v}{\frac{GR^2}{4\mu}} \qquad Q_D = \frac{8Q\mu}{\pi R^4 G}$$

$$v_D(r_D, t_D) = 1 - {r_D}^2 - 8\sum_{n=1}^{\infty} \frac{J_0(\lambda_n r_D)}{{\lambda_n}^3 J_1(\lambda_n)} \exp(-{\lambda_n}^2 t_D)$$

$$Q_D = 1 - 32\sum_{n=1}^{\infty} \frac{1}{{\lambda_n}^4} \exp(-{\lambda_n}^2 t_D)$$

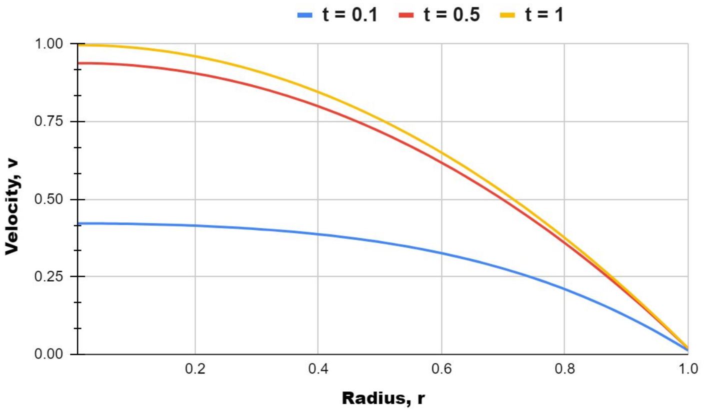

Fig. 7. Dimensionless velocity profile

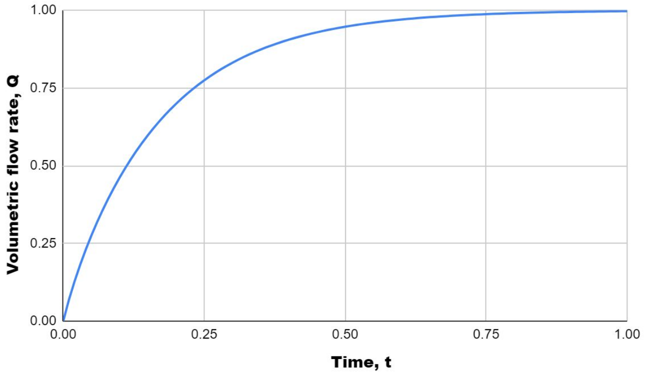

Fig. 8. Dimensionless flow rate

Analytical solution (Turbulent)

Turbulent case

$$Re = \frac{vD\rho}{\mu} > 2200$$

Darcy–Weisbach equation

$$G = \frac{\rho v^2}{2} \cdot \frac{f(Re)}{D}$$

Semi empirical turbulent profile

$$v = v^* \left[2.5 \cdot ln\left(\frac{R-r}{\nu} v^*\right) + 5\right] \qquad v^* = \sqrt{\frac{\tau_w}{\rho}} = \sqrt{\frac{R}{2} \cdot G \cdot \frac{1}{\rho}}$$

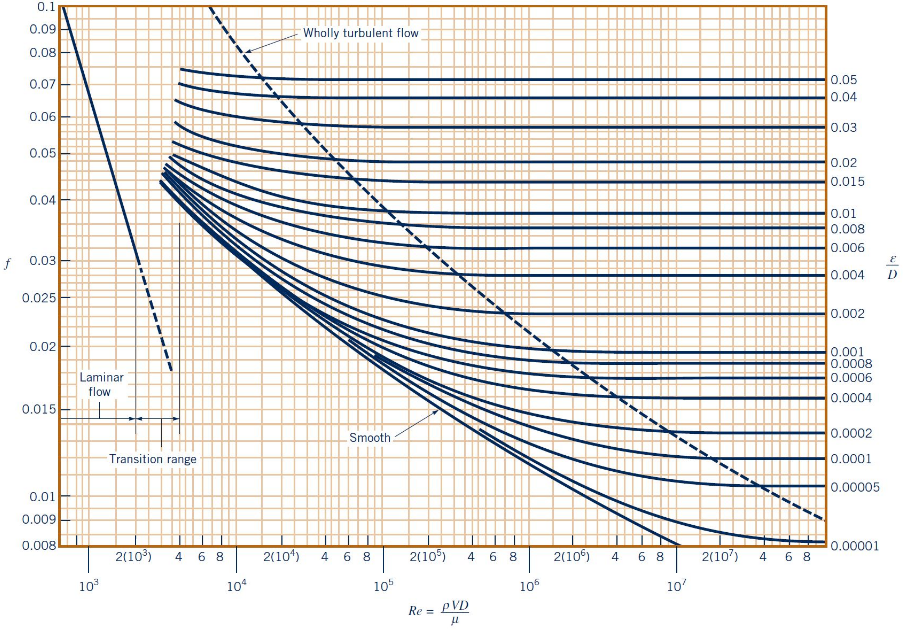

Fig. 9. Moody's chart.

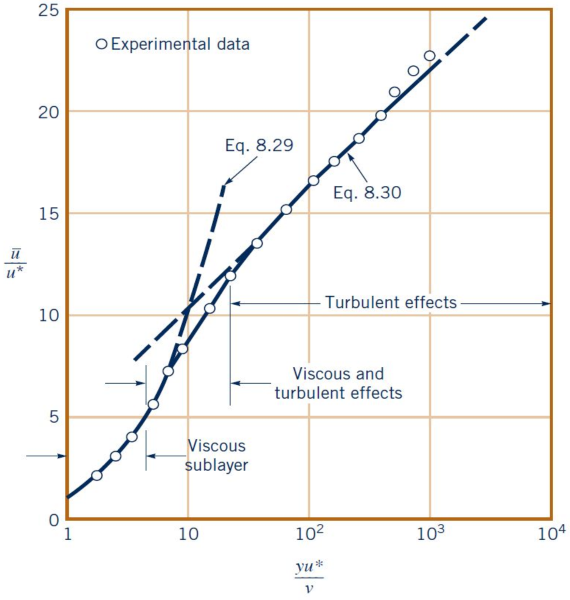

Fig. 10. Typical structure of a turbulent profile in a pipe.

Analytical solution (Turbulent)

Turbulent case

$$Re = \frac{vD\rho}{\mu} > 2200$$

Darcy–Weisbach equation

$$G = \frac{\rho v^2}{2} \cdot \frac{f(Re)}{D}$$

Semi empirical turbulent profile

$$v = v^* \left[2.5 \cdot ln\left(\frac{R-r}{\nu} v^*\right) + 5\right] \qquad v^* = \sqrt{\frac{\tau_w}{\rho}} = \sqrt{\frac{R}{2} \cdot G \cdot \frac{1}{\rho}}$$

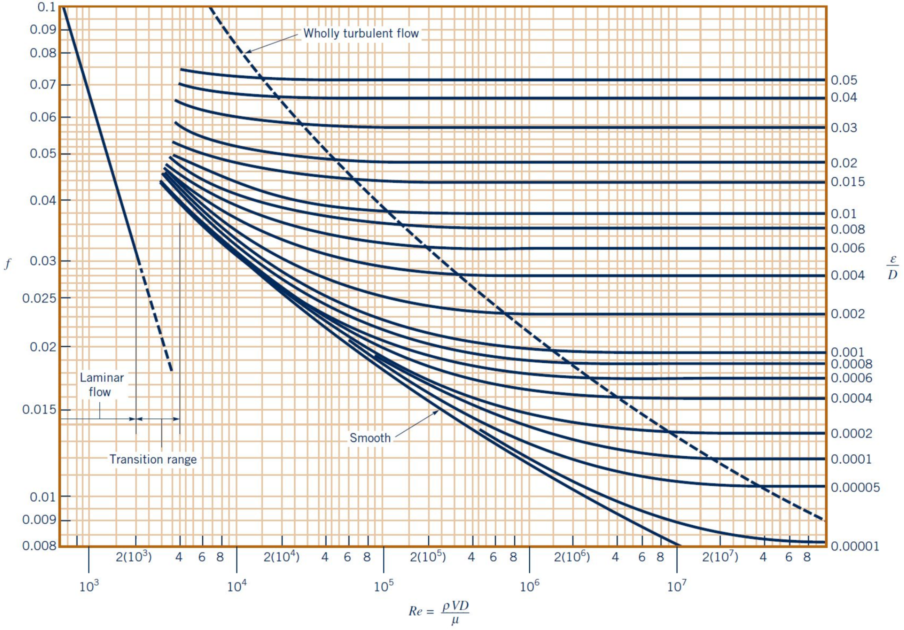

Fig. 9. Moody's chart.

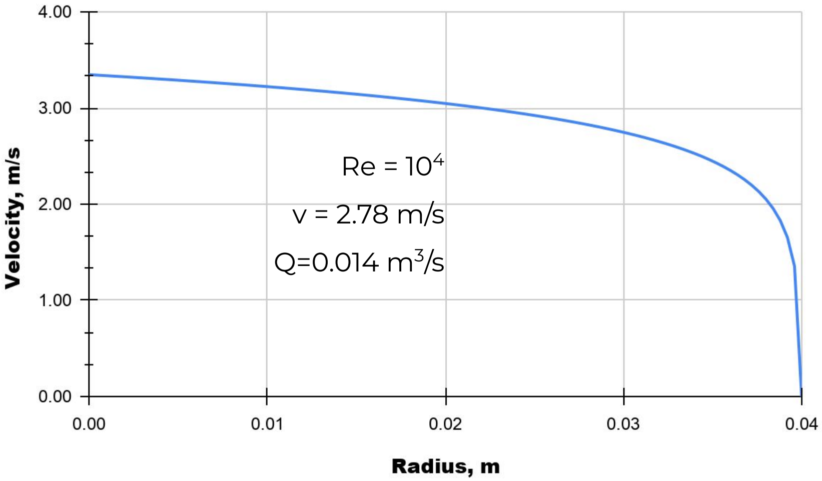

Fig. 11. Turbulent velocity profile based on semi-empirical formula.

Numerical solution - Ansys. Problem statement

Laminar Flow: Re 100

Model: Laminar; Transient

Boundary Conditions:
- ➔ Inlet - Gauge Pressure 3.3 Pa
- ➔ Outlet - Gauge Pressure 0 Pa
- ➔ Wall - No Slip

Initial condition - computed form inlet:
At t = 0 Pressure is applied to the inlet.

Transition Flow: Re 2200

Model: k-e standard; Steady

Boundary Conditions:
- ➔ Inlet - Gauge Pressure 73.3 Pa
- ➔ Outlet - Gauge Pressure 0 Pa
- ➔ Wall - No Slip

Initial condition - computed form inlet:
At t = 0 Pressure is applied to the inlet.

Turbulent Flow: Re 10000

Model: k-e standard; Transient

Boundary Conditions:
- ➔ Inlet - Gauge Pressure 1614 Pa
- ➔ Outlet - Gauge Pressure 0 Pa
- ➔ Wall - No Slip

Initial condition - computed form inlet:
At t = 0 Pressure is applied to the inlet.

Numerical solution - Ansys. Mesh Sensitivity

Table 2. Mesh sensitivity study for ANSYS

Elements	Mesh	Max Velocity m/s	Difference, %
106800	El.S - 11 mm, Edge - 4mm	1.8457347	
224400	El.S - 9 mm, Edge - 3mm	1.795509	2.76
464165	El.S - 7 mm, Edge - 2.5mm	1.7408091	3.09
912600	El.S - 5 mm, Edge - 2mm	1.7038741	2.14

Notes:

- ➔ 4 mesh sizes were studied + mesh with inflation
- ➔ Computational time with inflation mesh elements increases dramatically
- ➔ Mesh was choosing through the compromise of computational time and solution accuracy

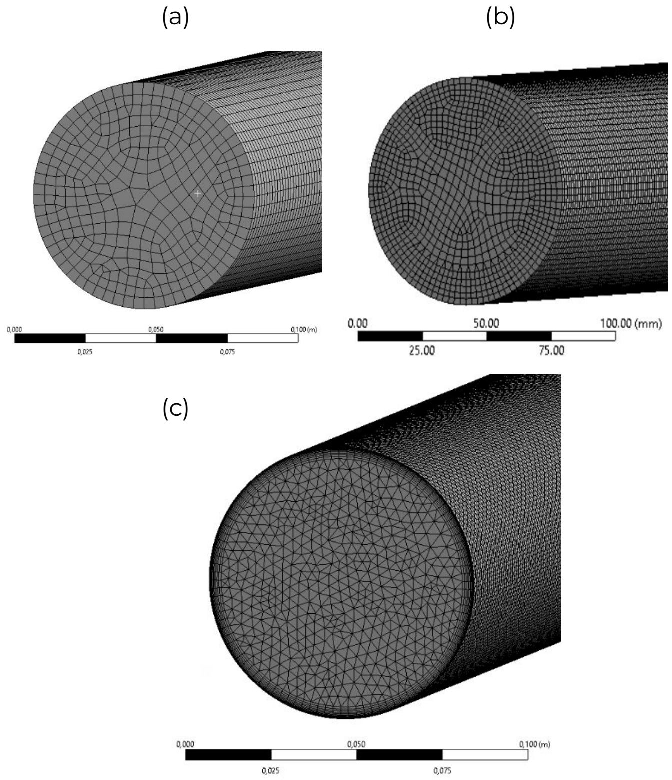

Fig. 12. Ansys mesh element size and edge size (a) 11 mm, (b) 7 mm, (c) 7 mm + inflation

Numerical solution - Ansys. Laminar flow

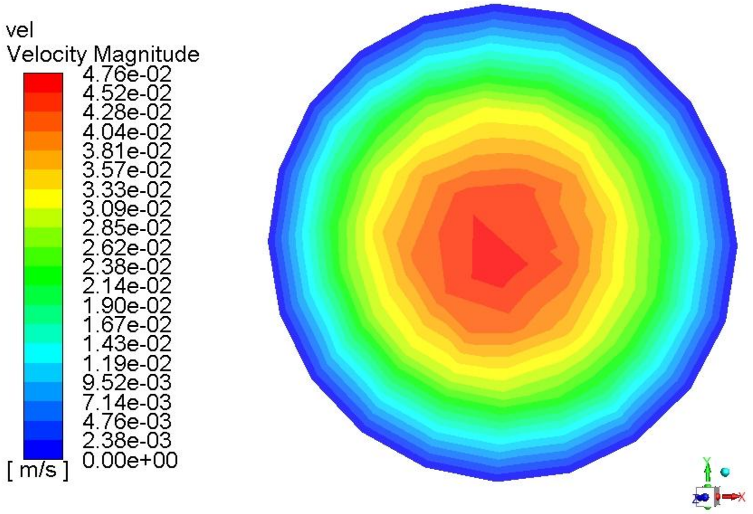

Fig. 13. Velocity magnitude contours for laminar flow.

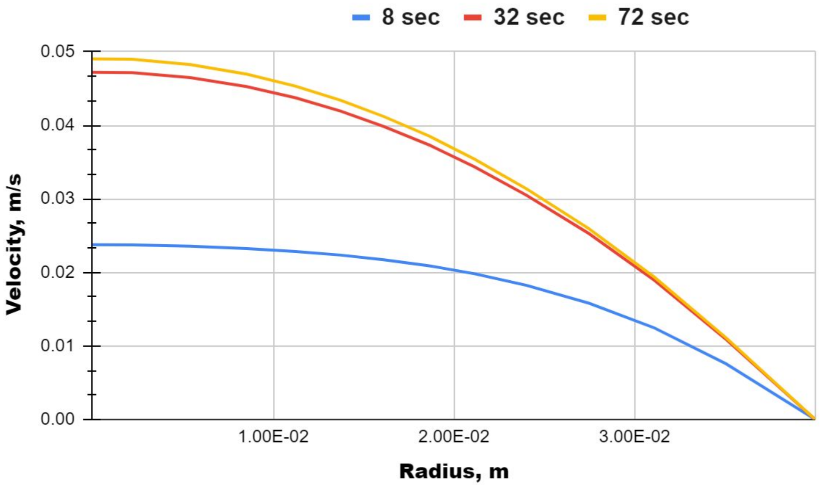

Fig. 14. Velocity profiles for different time in laminar flow.

Fig. 15. Velocity magnitude distribution along the pipe within laminar flow.

Numerical solution - Ansys. Transient flow

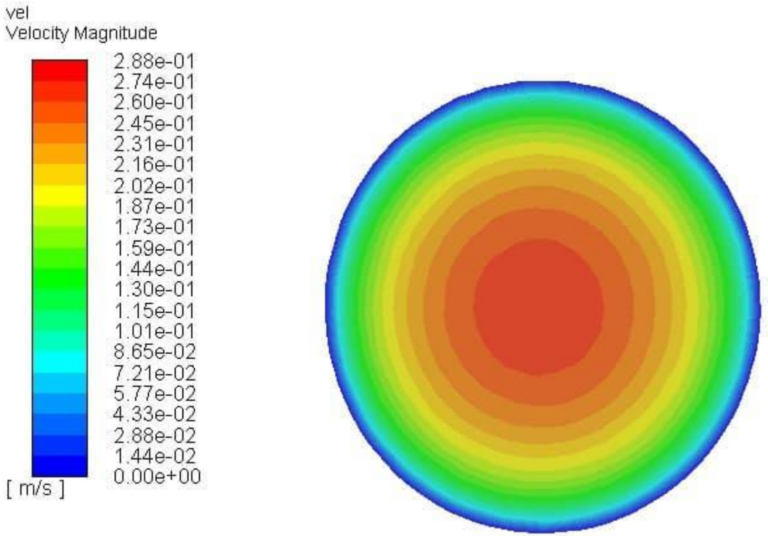

Fig. 16. Velocity magnitude contours for transient flow.

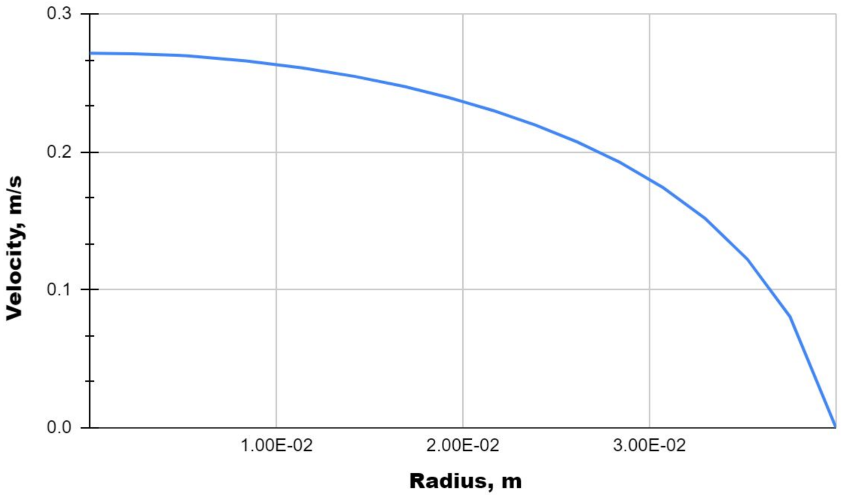

Fig. 17. Velocity profiles for different time in transient flow.

Fig. 18. Velocity magnitude distribution along the pipe within transient flow.

Numerical solution - Ansys. Turbulent flow

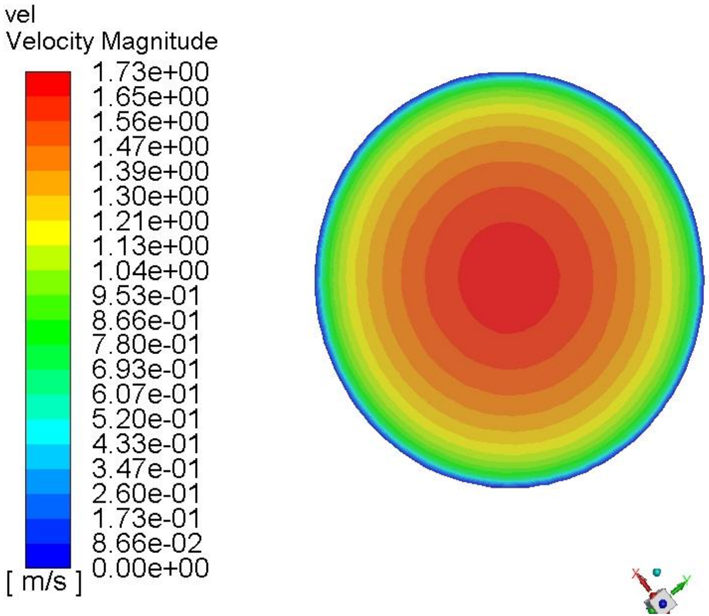

Fig. 19. Velocity magnitude contours for turbulent flow.

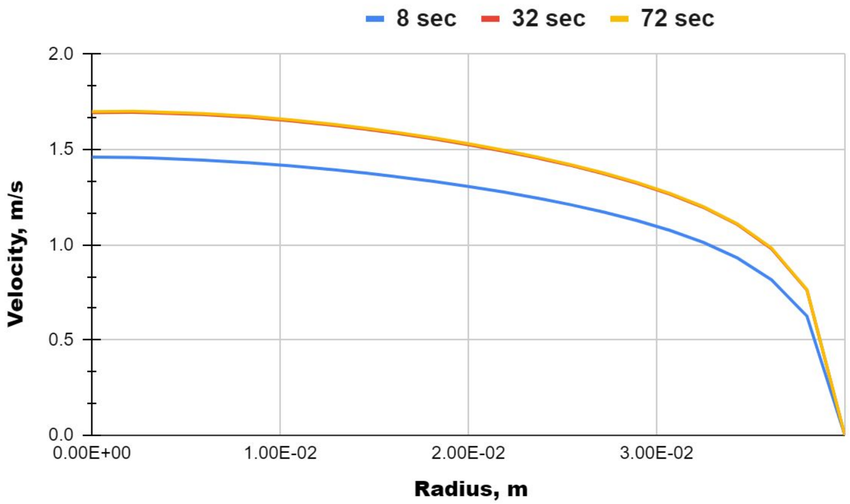

Fig. 20. Velocity profiles for different time in turbulent flow.

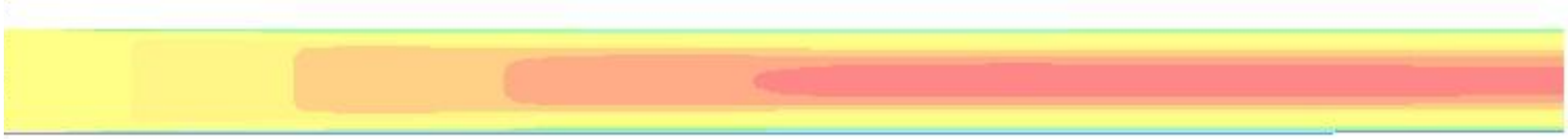

Fig. 21. Velocity magnitude distribution along the pipe within turbulent flow.

Numerical solution - Ansys. Flow comparison.

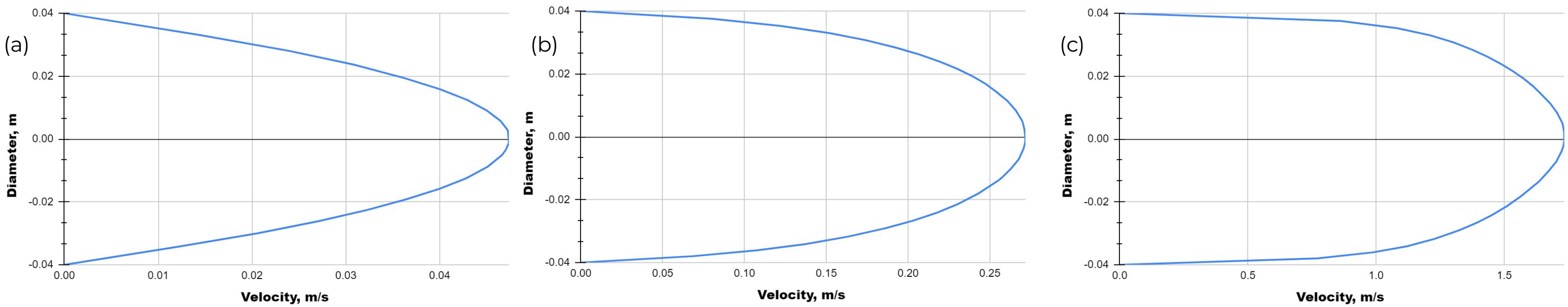

Fig. 22. Velocity profiles for (a) laminar, (b) transient and (c) turbulent flows.

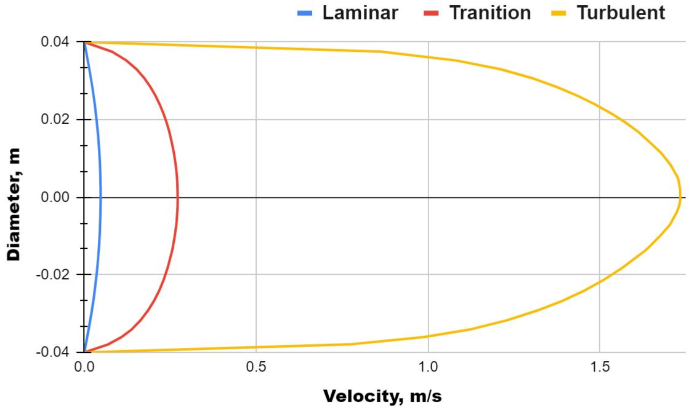

Fig. 23. Velocity profiles comparison.

Notes:

- ➔ 3 values of Re were considered to study the velocity flow profile development
- ➔ Velocity profile development is observes as we increase the Re

Numerical Solution: FlowVision - Statement

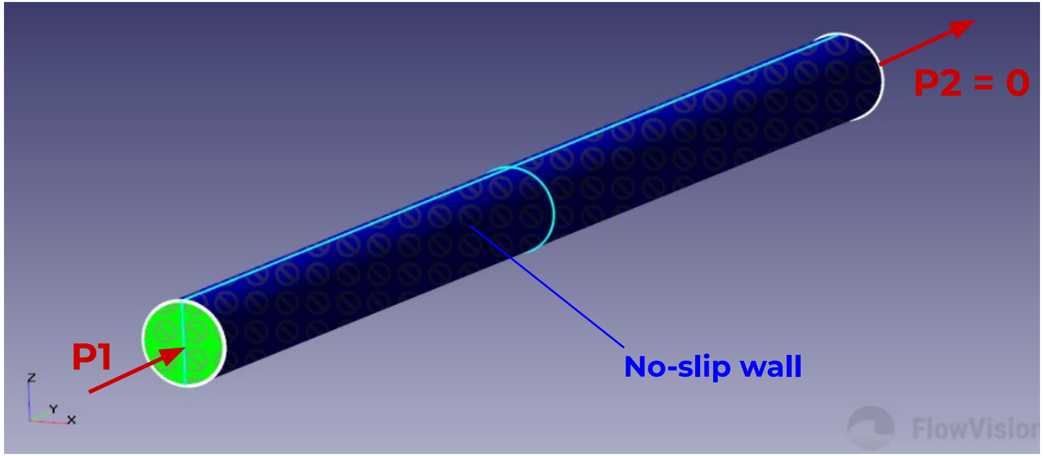

Fig. 24. FlowVision statement initial and boundary conditions.

Table 3. FlowVision problem initial data.

Characteristic	Value
ρ, kg/m^3	900
μ, kg/(m-s)	0.02
Laminar P1, Pa	3.3
Turbulent P1, Pa	1614

Numerical Solution: FlowVision - Mesh Sensitivity

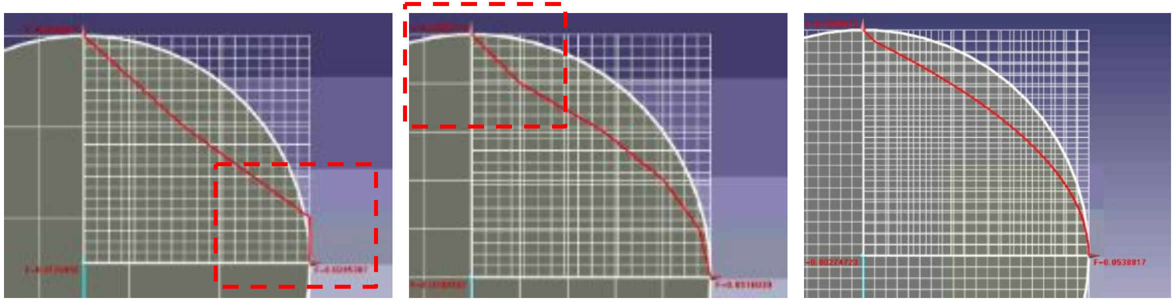

Fig. 25. Velocity profile for different mesh.

Table 4. Mesh sensitivity study for FlowVision

Cells	Mesh	Q, m3/s	Difference, %
1050	5x50x5	0.000157	
8800	10x100x10	0.0001448	8.08
66400	20x200x20	0.0001387	4.30
219600	30x300x30	0.0001367	1.45
515200	40x400x40	0.0001358	0.66
480800	**20x200x20 with wall adaptation**		

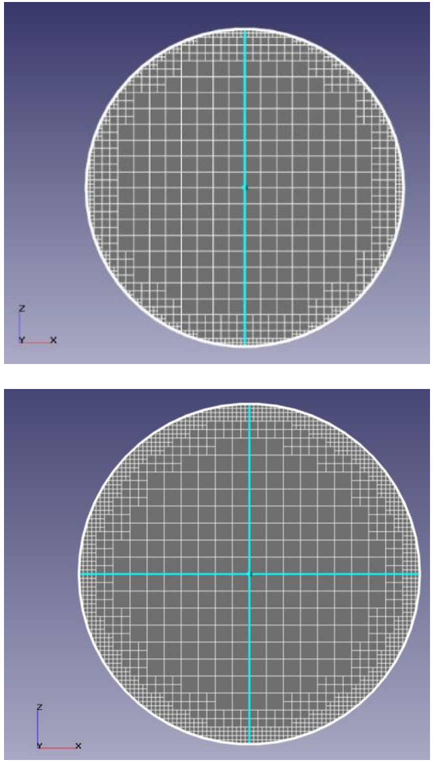

Fig. 26. Suitable mesh option with adaptation near the wall boundary.

Numerical Solution: FlowVision - Results

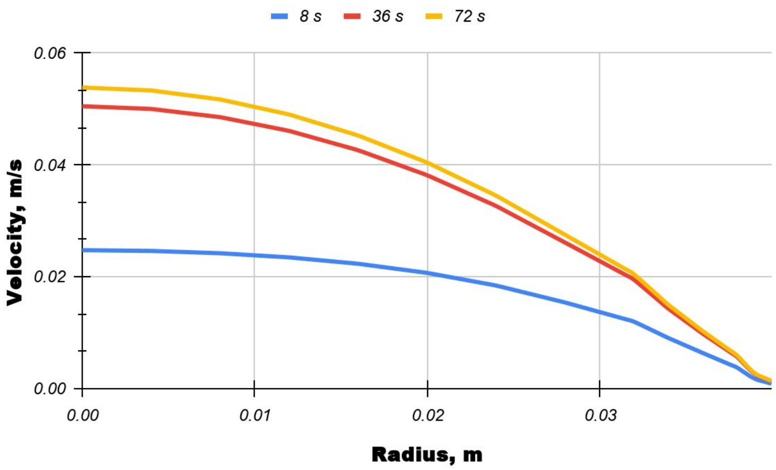

Fig. 27. Velocity profile for different time moments.

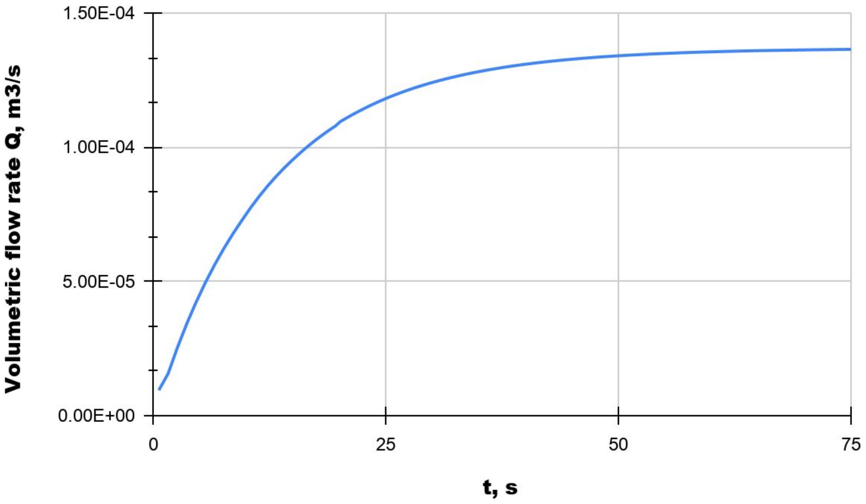

Fig. 28. Development of volumetric flow rate in time.

Numerical Solution: FlowVision - Results

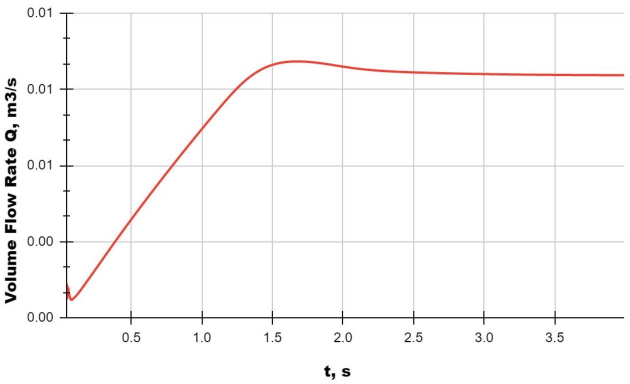

Fig. 30. Development of volumetric flow rate in time (turbulent k-ε model).

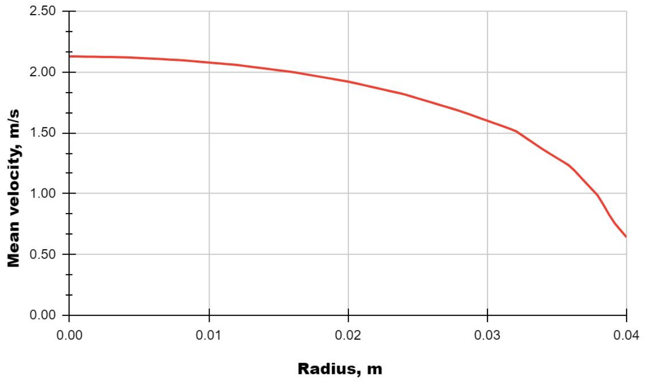

Fig. 31. Velocity profile (turbulent k-ε model).

Table 5. Turbulent model recommendation

Y^+	Подход	Модели турбулентности	Пристеночные функции
$Y^+<1$	Низко Re	KEFV, KEAKN, SA, SST	нет
$2<Y^+<5$	мертвая зона	Нет. при $Y^+>4$ можно попробовать KEFV	- неравновесные
$Y^+>5$	Высоко Re	KEFV	неравновесные
$Y^+>15$	Высоко Re	KEFV, SST	равновесные
$Y^+>30$	Высоко Re	KEFV, KES, SA, KEQ, SST, Sm.	равновесные

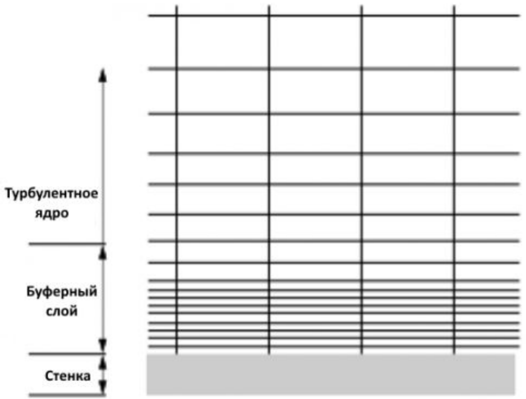

Results & Discussion

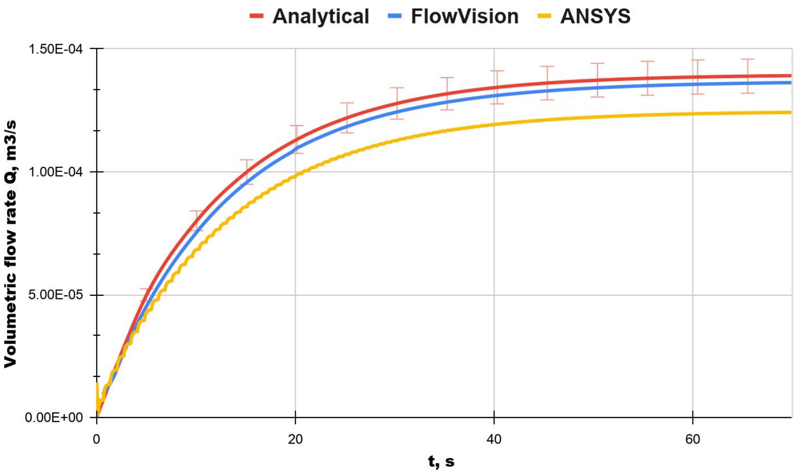

Fig. 32. Volumetric flow rate development for Analytical and Numerical solutions (FlowVision/ANSYS)

Notes:

- ➔ 3 moments of time considered, 72 s - time of developed flow
- ➔ Fine correlation of Analytical and FlowVision results
- ➔ ANSYS demonstrates > 10 % difference: boundary effects

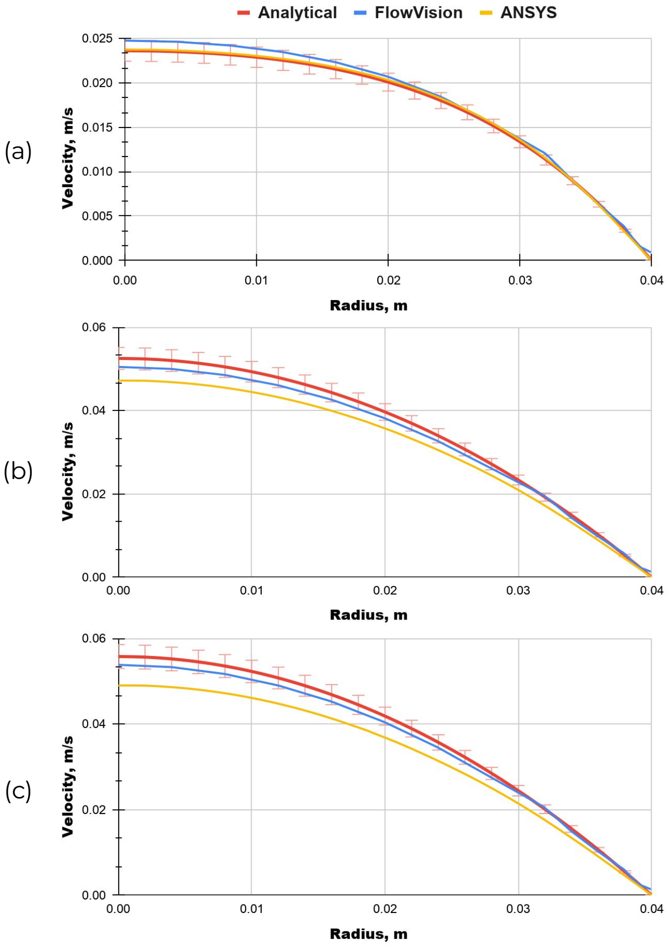

Fig. 33. Velocity profiles at time (a) 8s, (b) 36s, (c) 72s for Analytical and Numerical solutions (FlowVision/ANSYS)

Results & Discussion

Table 6. Deviation of FV & ANSYS solution comparing to Analytical

Time	8 s	36 s	72 s
FV (laminar)	4.83 %	3.87 %	3.47 %
Ansys (laminar)	0.54 %	10.15 %	12.14 %

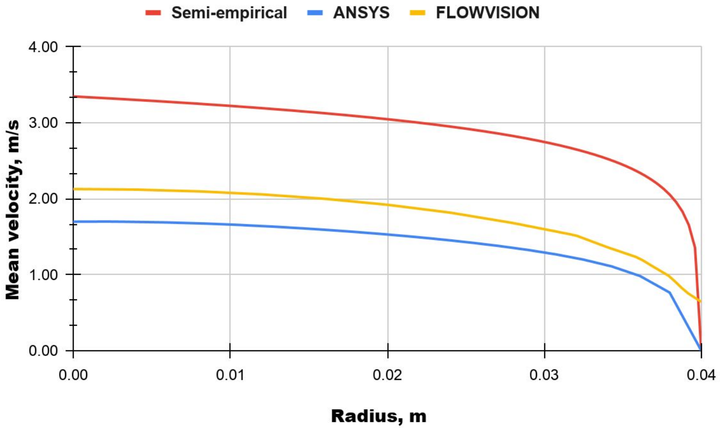

Fig. 34. Velocity profile comparison for developed turbulent flow.

- ➔ Numerical solution both for FlowVision and Ansys showed appropriately fine results for laminar flow and considerable difference with turbulent solution due to semi-empirical approach;
- ➔ Possible reasons for the ANSYS software might be the loss due to rough mesh or unexpected friction losses;
- ➔ Different numerical solvers and meshing algorithms might affect the final solution and should be further studied;

Discussion & Future Efforts

- ➔ Effects of boundary conditions were observed. One can see that maximum deviation for FlowVision is decreasing over time with value less than 3.5 % when for ANSYS it is growing and can reach up to 12 % due to the boundary effects which should be further studied which takes significant computational time.
- ➔ A specific friction coefficient shall be taken in account and compared to provide more physical result for solution. Friction on the wall characteristic shall be compared for convergence analysis.
- ➔ ANSYS and FlowVision shows great results in simulating turbulent flow. Based on observed results, FlowVision seems as a promising study tool giving the best accuracy comparing with analytical solution.

Thank you for attention!

Anastasia Cumika, 2nd year MSc student, CDMM

Oleg Nikolaev, 1st year MSc student, CHR

Ruslan Vorobyev, 3rd year PhD student, CDMM

Skoltech

Skolkovo Institute of Science and Technology